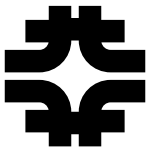

Fermi National Accelerator Laboratory

FERMILAB-Pub-95/383-A

A Fast and Accurate Algorithm for Computing Tensor CBR Anisotropy

M.S. Turner and Y. Wang

Fermi National Accelerator Laboratory
P.O. Box 500, Batavia, Illinois 60510

December 1995

Submitted to *Physical Review D*

Operated by Universities Research Association Inc. under Contract No. DE-AC02-76CHO3000 with the United States Department of Energy

Disclaimer

FERMILAB-Pub-95/383-A
astro-ph/9512140
Submitted to *Physical Review D*
December 1995

A FAST AND ACCURATE ALGORITHM FOR COMPUTING TENSOR CBR ANISOTROPY

Michael S. Turner[1,2] and Yun Wang[1]

[1] *NASA/Fermilab Astrophysics Center*

Fermi National Accelerator Laboratory, Batavia, IL 60510-0500

Departments of Physics and of Astronomy & Astrophysics, Enrico Fermi Institute

The University of Chicago, Chicago, IL 60637-1433

Abstract

Inflation gives rise to a nearly scale-invariant spectrum of tensor perturbations (gravitational waves), their contribution to the Cosmic Background Radiation (CBR) anisotropy depends upon the present cosmological parameters as well as inflationary parameters. The analysis of a sampling-variance-limited CBR map offers the most promising means of detecting tensor perturbations, but will require evaluation of the predicted multipole spectrum for a very large number of cosmological parameter sets. We present accurate polynomial formulae for computing the predicted variance of the multipole moments in terms of the cosmological parameters Ω_Λ, $\Omega_0 h^2$, $\Omega_B h^2$, N_ν, and the power-law index n_T which are accurate to about 1% for $l \leq 50$ and to better than 3% for $50 < l \leq 100$ (as compared to the numerical results of a Boltzmann code).

PACS index numbers: 04.30.+x, 98.80.Cq, 98.80.Es

I. Introduction

Inflation makes three robust predictions: flat Universe and nearly scale-invariant spectra of scalar (density) and tensor (gravitational-wave) metric perturbations [1]. The scalar [2] and tensor [3] perturbations arise from quantum mechanical fluctuations on very small scales during inflation and are stretched to astrophysically interesting scales by the tremendous growth of the cosmic scale factor during inflation.

Both the scalar and tensor perturbations give rise to anisotropy in the temperature of the Cosmic Background Radiation (CBR) seen on the sky today, most conveniently described by their contribution to the multipole decomposition of the CBR temperature

$$\delta T(\theta,\phi)/T = \sum_{l=2}^{\infty}\sum_{m=-l}^{l} a_{lm}Y_{lm}(\theta,\phi). \tag{1.1}$$

The scalar and tensor contributions to the anisotropy predicted by inflation are uncorrelated and statistical in character. The individual multipoles that describe our sky are given by the sum of a scalar plus tensor contribution, with these contributions being drawn from gaussian distributions with variances $\langle|a_{lm}^S|^2\rangle$ and $\langle|a_{lm}^T|^2\rangle$, which are related to the properties of the inflationary potential and cosmological parameters. Because the scalar and tensor contributions are uncorrelated, the variance $\langle|a_{lm}|^2\rangle = \langle|a_{lm}^S|^2\rangle + \langle|a_{lm}^T|^2\rangle$. The expected scalar [4] and tensor contributions are shown in Fig. 1 for a nominal set of cosmological parameters.

CBR anisotropy offers a very promising means of testing inflation as well as determining the scalar and tensor perturbations. If both can be measured, then information about the underlying inflationary potential can be derived (value of the potential and its first few derivatives at a point) [5]. Key to doing this is a high-angular-resolution (better than 0.5°), sampling-variance-limited map of the CBR sky. (Because there are only $2l+1$ multipoles, sampling variance limits the accuracy to which $\langle|a_{lm}|^2\rangle$ can be measured – a relative precision of $\sqrt{2/(2l+1)}$.) Three proposals have been made to NASA (FIRE, PSI,

and MAP) for a satellite-borne experiment and another to ESA (COBRAS/SAMBA). A satellite could be launched as early as 1999.

The separation of the scalar and tensor contributions to CBR anisotropy is likely to be done by maximum likelihood techniques and will require accurate predictions for the scalar and tensor contributions (1% or better) to the anisotropy for many sets of cosmological and inflationary parameters. At present, achieving such precision requires numerically integrating Boltzmann equations, which is very time consuming (typically requiring many hours on a powerful workstation for one set of cosmological parameters) [6]. The need for a fast and accurate approximation scheme is manifest.

Many analytic approximations to the tensor angular power spectrum have been explored [7]. The most accurate is as time consuming as numerically integrating the Boltzmann equations [8], and even schemes with less accuracy require significant computation time (tens of minutes). This motivated the present approach – a polynomial fit that can be evaluated very rapidly (much less than a second for a set of cosmological parameters).

The tensor angular power spectrum, $C_l(\boldsymbol{P}) = \langle |a_{lm}^T|^2 \rangle$, depends upon a set of cosmological and inflationary parameters denoted here by $\boldsymbol{P}$. The set $\boldsymbol{P}$ is: the baryon density, $\Omega_B h^2$; the matter density, $\Omega_0 h^2$; the level of radiation in the Universe, parameterized by the equivalent number of massless neutrino species N_ν; the present vacuum-energy density, $\Omega_\Lambda \equiv 1 - \Omega_0$; and the primordial power-law index of the tensor perturbations, n_T ($n_T = 0$ for scale invariant tensor perturbations). We will only be concerned with the shape of the angular power spectrum; the overall amplitude of the angular power spectrum, conveniently specified by C_2, depends upon the inflationary parameters (the value of the inflationary potential in Planck units) as described elsewhere [9]. In most approaches, the shape (C_l/C_2) and the overall amplitude (C_2) are determined independently.

The dependence upon the parameters is simple to explain. The shape of the angu-

lar power spectrum depends on the redshift of last scattering and the evolution of the gravitational waves after they enter the horizon, which depends upon the evolution of the cosmic scale factor. The redshift of last scattering (more precisely, the peak of the visibility function; see Appendix B) depends upon the baryon density, the matter density, and the level of radiation in the Universe. The evolution of the scale factor of the Universe around last scattering depends upon the relative levels of matter and radiation through the value of the scale factor at matter-radiation equality,

$$R_{\rm EQ} = 4.16 \times 10^{-5} (\Omega_0 h^2)^{-1} \left(\frac{2 + 0.4542 N_\nu}{3.3626} \right) . \tag{1.2}$$

The recent evolution of the scale factor, which depends upon Ω_Λ as well, is also important for gravitational wave modes which have recently entered the horizon and influence the low l multipoles. Finally, the primordial spectral shape of tensor perturbations (described by n_T) also affects the shape of the angular power spectrum.

We have engineered our fits based upon the numerical results of the Boltzmann code written by Dodelson and Knox [10]; they believe that their code is accurate to better than 1%. We expand $C_l(\boldsymbol{P})$ around a fiducial set of parameters: for $\Omega_\Lambda = 0$ ($\Omega_0 = 1$), $h = 0.5$, $N_\nu = 3$, $\Omega_B h^2 = 0.0125$, and $n_T = 0$; and for $\Omega_\Lambda \neq 0$, $\Omega_0 h^2 = 0.125$, $\Omega_B h^2 = 0.0125$, $\Omega_\Lambda = 0.5$, $N_\nu = 3$ and $n_T = 0$. These two cases are treated in the next two Sections. We end with a brief discussion of the accuracy of our fits.

II. Zero Cosmological Constant

For $\Omega_\Lambda = 0$, the cosmological parameters are $(h, N_\nu, \Omega_B h^2, n_T)$. We define a parameter vector, $\boldsymbol{P} = ([h\, f(N_\nu)], N_\nu, [\Omega_B h^2]^{-1}, n_T)$, where

$$f(N_\nu) = \sqrt{\frac{3.3626}{2 + 0.4542\, N_\nu}}, \tag{2.1}$$

which is related to $R_{\rm EQ}$ of Eq.(1.2).

We expand the tensor multipole spectrum for $\boldsymbol{P}$ around the tensor multipole spectrum for $\boldsymbol{P} = \boldsymbol{Q} \equiv (0.5, 3, 80, 0)$ [which corresponds to $h = 0.5, N_\nu = 3, \Omega_B h^2 = 0.0125$, and $n_T = 0$]. We write

$$\frac{C_l(\boldsymbol{P})}{C_2(\boldsymbol{P})} = \frac{C_l(\boldsymbol{Q})}{C_2(\boldsymbol{Q})} \left(\frac{l}{2}\right)^{n_T} [1 + g(l)\, n_T] \left\{ \frac{1 + \sum_{i=1}^{3} f_i(P_i - Q_i, l)}{1 + \sum_{i=1}^{3} f_i(P_i - Q_i, 2)} \right\}. \tag{2.2}$$

where

$$\begin{aligned} f_1(P_1 - Q_1, l) &= \sum_{j=1}^{4} a_j(l)\, (P_1 - Q_1)^j \\ f_2(P_2 - Q_2, l) &= \sum_{j=1}^{3} b_j(l)\, (P_2 - Q_2)^j \\ f_3(P_3 - Q_3, l) &= \sum_{j=1}^{3} d_j(l)\, (P_3 - Q_3)^j \end{aligned} \tag{2.3}$$

The coefficients are found numerically by fitting to the variation due to each parameter separately. Identifying the relevant vector of parameters minimizes the need for cross terms.

The P_1 coefficients are

$$\begin{aligned} a_1(l) &= -0.4025 \left(\frac{l}{100}\right) - 0.3375 \left(\frac{l}{100}\right)^2 - 2.3441 \left(\frac{l}{100}\right)^3 + 2.0125 \left(\frac{l}{100}\right)^4 \\ a_2(l) &= 1.1271 \left(\frac{l}{100}\right) - 2.0614 \left(\frac{l}{100}\right)^2 + 10.9105 \left(\frac{l}{100}\right)^3 - 10.8102 \left(\frac{l}{100}\right)^4 \\ a_3(l) &= -2.7875 \left(\frac{l}{100}\right) + 10.9417 \left(\frac{l}{100}\right)^2 - 36.4181 \left(\frac{l}{100}\right)^3 + 41.1617 \left(\frac{l}{100}\right)^4 \\ a_4(l) &= 3.4719 \left(\frac{l}{100}\right) - 16.8888 \left(\frac{l}{100}\right)^2 + 51.2793 \left(\frac{l}{100}\right)^3 - 61.1775 \left(\frac{l}{100}\right)^4. \end{aligned} \tag{2.4}$$

The P_2 coefficients are

$$\begin{aligned} b_1(l) &= 10^{-3} \left[-0.0361 \left(\frac{l}{100}\right) + 5.3684 \left(\frac{l}{100}\right)^2 + 3.3680 \left(\frac{l}{100}\right)^3 \right. \\ &\qquad \left. -2.0872 \left(\frac{l}{100}\right)^4 + 1.2639 \left(\frac{l}{100}\right)^5 \right] \end{aligned}$$

$$
\begin{aligned}
b_2(l) &= 10^{-3}\left[-0.1105\left(\frac{l}{100}\right)+0.1237\left(\frac{l}{100}\right)^2-1.8853\left(\frac{l}{100}\right)^3\right. \\
&\qquad \left.+2.2411\left(\frac{l}{100}\right)^4-1.0243\left(\frac{l}{100}\right)^5\right] \\
b_3(l) &= 10^{-4}\left[0.1297\left(\frac{l}{100}\right)-0.5125\left(\frac{l}{100}\right)^2+2.3069\left(\frac{l}{100}\right)^3\right. \\
&\qquad \left.-2.9658\left(\frac{l}{100}\right)^4+1.5493\left(\frac{l}{100}\right)^5\right].
\end{aligned}
\tag{2.5}
$$

The P_3 coefficients are

$$
\begin{aligned}
d_1(l) &= 10^{-4}\left[-0.1972\left(\frac{l}{100}\right)+12.3357\left(\frac{l}{100}\right)^2-0.7469\left(\frac{l}{100}\right)^3+4.0362\left(\frac{l}{100}\right)^4\right] \\
d_2(l) &= 10^{-6}\left[-0.0241\left(\frac{l}{100}\right)-1.7123\left(\frac{l}{100}\right)^2-1.1385\left(\frac{l}{100}\right)^3+0.6791\left(\frac{l}{100}\right)^4\right] \\
d_3(l) &= 10^{-10}\left[0.2028\left(\frac{l}{100}\right)+12.3878\left(\frac{l}{100}\right)^2+8.9878\left(\frac{l}{100}\right)^3-6.1211\left(\frac{l}{100}\right)^4\right].
\end{aligned}
\tag{2.6}
$$

The coefficient involving n_T is

$$
\begin{aligned}
g(l) &= -0.4764\left[1-e^{-(l-2)/30}\right]+1.6734\left[1-e^{-2(l-2)/30}\right]-4.0400\left[1-e^{-3(l-2)/30}\right] \\
&\qquad +4.6345\left[1-e^{-4(l-2)/30}\right]-2.2942\left[1-e^{-5(l-2)/30}\right].
\end{aligned}
\tag{2.7}
$$

III. Nonzero Cosmological Constant

For $\Omega_\Lambda > 0$, the cosmological parameters are ($\Omega_0 h^2$, $\Omega_B h^2$, Ω_Λ, N_ν, n_T). The procedure of fitting is similar to the $\Omega_\Lambda = 0$ case, but slightly more complicated because one "cross term" is required to achieve sufficient accuracy.

Here we define the parameter vector, $\boldsymbol{P} = \left(\left[f(N_\nu)\sqrt{\Omega_0 h^2}\right], N_\nu, [\Omega_B h^2]^{-1}, \Omega_\Lambda, n_T\right)$. Again, we expand the C_l's for $\boldsymbol{P}$ around the C_l's for a standard set of cosmological

parameters, $\boldsymbol{S}$. For $\Omega_\Lambda < 0.36$, we take $\boldsymbol{S} = (0.5, 3, 80, 0, 0)$ [which corresponds to $h = 0.5, N_\nu = 3, \Omega_B h^2 = 0.0125, \Omega_\Lambda = 0$, and $n_T = 0$]. For $0.36 \leq \Omega_\Lambda \leq 0.8$, we take $\boldsymbol{S} = (0.3536, 3, 80, 0.5, 0)$ [which corresponds to $h = 0.5, N_\nu = 3, \Omega_B h^2 = 0.0125, \Omega_\Lambda = 0.5$, and $n_T = 0$]. As before, we write

$$\frac{C_l(\boldsymbol{P})}{C_2(\boldsymbol{P})} = \frac{C_l(\boldsymbol{S})}{C_2(\boldsymbol{S})} \left(\frac{l}{2}\right)^{n_T} [1 + \nu(l)\, n_T] \left\{ \frac{1 + \sum_{i=1}^4 f_i(P_i - S_i, l) + \eta(l)(P_1 - S_1)(P_4 - S_4)}{1 + \sum_{i=1}^4 f_i(P_i - S_i, 2) + \eta(2)(P_1 - S_1)(P_4 - S_4)} \right\}, \tag{3.1}$$

where

$$\begin{aligned} f_1(P_1 - S_1, l) &= \sum_{j=1}^4 A_j(l)\,(P_1 - S_1)^j \\ f_2(P_2 - S_2, l) &= \sum_{j=1}^3 B_j(l)\,(P_2 - S_2)^j \\ f_3(P_3 - S_3, l) &= \sum_{j=1}^3 D_j(l)\,(P_3 - S_3)^j \\ f_4(P_4 - S_4, l) &= \sum_{j=1}^4 E_j(l)\,(P_4 - S_4)^j, \end{aligned} \tag{3.2}$$

For $\Omega_\Lambda < 0.36$,

$$\begin{aligned} &A_j(l) = a_j(l), \quad B_j(l) = b_j(l), \quad D_j(l) = d_j(l); \\ &\nu(l) = g(l), \quad \eta(l) = 0. \end{aligned} \tag{3.3}$$

The P_4 coefficients are

$$\begin{aligned} &E_1(2) = -6.0163 \times 10^{-2}, \quad E_1(3) = -1.4845 \times 10^{-2}, \quad E_1(4) = -4.3594 \times 10^{-3} \\ &E_2(2) = -3.2853 \times 10^{-2}, \quad E_2(3) = -8.4852 \times 10^{-3}, \quad E_2(4) = -2.5631 \times 10^{-3} \\ &E_3(2) = -1.8426 \times 10^{-2}, \quad E_3(3) = -4.0997 \times 10^{-3}, \quad E_3(4) = -9.4267 \times 10^{-4} \\ &E_4(2) = -2.8162 \times 10^{-2}, \quad E_4(3) = -8.6348 \times 10^{-3}, \quad E_4(4) = -3.1561 \times 10^{-3} \end{aligned}$$

$$E_1(l > 4) = 0.1 \left[0.1483 \left(\frac{l}{100}\right) - 2.4098 \left(\frac{l}{100}\right)^2 + 0.3211 \left(\frac{l}{100}\right)^3 - 0.6630 \left(\frac{l}{100}\right)^4 \right]$$

$$
\begin{aligned}
E_2(l>4) &= 0.1\left[0.0768\left(\frac{l}{100}\right)-1.5272\left(\frac{l}{100}\right)^2-0.2895\left(\frac{l}{100}\right)^3+0.1754\left(\frac{l}{100}\right)^4\right] \\
E_3(l>4) &= 0.1\left[0.0580\left(\frac{l}{100}\right)-1.0585\left(\frac{l}{100}\right)^2-0.1897\left(\frac{l}{100}\right)^3+0.2662\left(\frac{l}{100}\right)^4\right] \\
E_4(l>4) &= 0.1\left[0.0560\left(\frac{l}{100}\right)-1.6921\left(\frac{l}{100}\right)^2-0.8962\left(\frac{l}{100}\right)^3+1.0897\left(\frac{l}{100}\right)^4\right].
\end{aligned}
\tag{3.4}
$$

All other coefficients have been given in the previous Section.

For $0.36 \leq \Omega_\Lambda \leq 0.8$, the P_1 coefficients are

$$
\begin{aligned}
A_1(l) &= -1.0313\left(\frac{l}{100}\right)+1.0270\left(\frac{l}{100}\right)^2-7.6262\left(\frac{l}{100}\right)^3 \\
&\quad +6.8176\left(\frac{l}{100}\right)^4-2.9419\left(\frac{l}{100}\right)^5 \\
A_2(l) &= 3.5896\left(\frac{l}{100}\right)-11.9704\left(\frac{l}{100}\right)^2+37.1339\left(\frac{l}{100}\right)^3 \\
&\quad -35.5609\left(\frac{l}{100}\right)^4+19.0353\left(\frac{l}{100}\right)^5 \\
A_3(l) &= -7.6185\left(\frac{l}{100}\right)+34.4566\left(\frac{l}{100}\right)^2-92.1698\left(\frac{l}{100}\right)^3 \\
&\quad +95.4331\left(\frac{l}{100}\right)^4-53.5697\left(\frac{l}{100}\right)^5 \\
A_4(l) &= 6.5272\left(\frac{l}{100}\right)-32.9224\left(\frac{l}{100}\right)^2+84.7298\left(\frac{l}{100}\right)^3 \\
&\quad -91.4209\left(\frac{l}{100}\right)^4+51.8163\left(\frac{l}{100}\right)^5.
\end{aligned}
\tag{3.5}
$$

The P_2 coefficients are

$$
\begin{aligned}
B_1(l) &= 10^{-2}\left[-0.1629\left(\frac{l}{100}\right)+1.4392\left(\frac{l}{100}\right)^2-2.2268\left(\frac{l}{100}\right)^3\right. \\
&\quad \left.+2.8450\left(\frac{l}{100}\right)^4-1.5396\left(\frac{l}{100}\right)^5\right] \\
B_2(l) &= 10^{-4}\left[0.3608\left(\frac{l}{100}\right)-6.3470\left(\frac{l}{100}\right)^2+3.4559\left(\frac{l}{100}\right)^3\right.
\end{aligned}
$$

$$
\begin{aligned}
& & -4.8620\left(\frac{l}{100}\right)^4 + 7.0136\left(\frac{l}{100}\right)^5\Bigg] \\
B_3(l) &= 10^{-4}\Bigg[0.1672\left(\frac{l}{100}\right) - 0.8800\left(\frac{l}{100}\right)^2 + 2.9272\left(\frac{l}{100}\right)^3 \\
& & -3.6758\left(\frac{l}{100}\right)^4 + 1.6453\left(\frac{l}{100}\right)^5\Bigg]. \qquad (3.6)
\end{aligned}
$$

The P_3 coefficients are

$$
\begin{aligned}
D_1(l) &= 10^{-4}\left[-0.1039\left(\frac{l}{100}\right) + 9.2599\left(\frac{l}{100}\right)^2 + 0.1085\left(\frac{l}{100}\right)^3 + 2.4910\left(\frac{l}{100}\right)^4\right] \\
D_2(l) &= 10^{-7}\left[-0.2716\left(\frac{l}{100}\right) - 16.4608\left(\frac{l}{100}\right)^2 - 11.4085\left(\frac{l}{100}\right)^3 + 8.5966\left(\frac{l}{100}\right)^4\right] \\
D_3(l) &= 10^{-9}\left[0.0962\left(\frac{l}{100}\right) + 2.8879\left(\frac{l}{100}\right)^2 + 3.0975\left(\frac{l}{100}\right)^3 - 3.0516\left(\frac{l}{100}\right)^4\right]. \qquad (3.7)
\end{aligned}
$$

The P_4 coefficients are

$$
\begin{aligned}
& E_1(2) = -1.3087\times10^{-1}, \quad E_1(3) = -3.1368\times10^{-2}, \quad E_1(4) = -8.4146\times10^{-3} \\
& E_2(2) = -1.1277\times10^{-1}, \quad E_2(3) = -2.7633\times10^{-2}, \quad E_2(4) = -7.3835\times10^{-3} \\
& E_3(2) = -1.3674\times10^{-1}, \quad E_3(3) = -3.4105\times10^{-2}, \quad E_3(4) = -8.9756\times10^{-3} \\
& E_4(2) = -6.8693\times10^{-1}, \quad E_4(3) = -1.7588\times10^{-1}, \quad E_4(4) = -4.5389\times10^{-2}
\end{aligned}
$$

$$
\begin{aligned}
E_1(l>4) &= 0.1\left[0.5211\left(\frac{l}{100}\right) - 5.7831\left(\frac{l}{100}\right)^2 + 1.0999\left(\frac{l}{100}\right)^3 - 1.2519\left(\frac{l}{100}\right)^4\right] \\
E_2(l>4) &= 0.1\left[0.4547\left(\frac{l}{100}\right) - 5.2202\left(\frac{l}{100}\right)^2 - 0.1399\left(\frac{l}{100}\right)^3 - 0.3364\left(\frac{l}{100}\right)^4\right] \\
E_3(l>4) &= 0.1\left[0.5924\left(\frac{l}{100}\right) - 7.3578\left(\frac{l}{100}\right)^2 - 1.5359\left(\frac{l}{100}\right)^3 + 1.3647\left(\frac{l}{100}\right)^4\right] \\
E_4(l>4) &= 0.5016\left(\frac{l}{100}\right) - 7.0197\left(\frac{l}{100}\right)^2 - 0.2120\left(\frac{l}{100}\right)^3 + 2.9141\left(\frac{l}{100}\right)^4. \qquad (3.8)
\end{aligned}
$$

The coefficient involving n_T is

$$\begin{aligned}\nu(l) &= -0.4670\left[1-e^{-(l-2)/30}\right]+1.7234\left[1-e^{-2(l-2)/30}\right]-4.2724\left[1-e^{-3(l-2)/30}\right] \\ &\quad +4.9757\left[1-e^{-4(l-2)/30}\right]-2.4571\left[1-e^{-5(l-2)/30}\right]. \qquad (3.9)\end{aligned}$$

Note that $\nu(l) \simeq g(l)$.

The cross-term coefficient is

$$\begin{aligned}\eta(l) &= -3.7201\left(\frac{l}{100}\right)+29.9770\left(\frac{l}{100}\right)^2-117.6372\left(\frac{l}{100}\right)^3+236.1950\left(\frac{l}{100}\right)^4 \\ &\quad -257.9630\left(\frac{l}{100}\right)^5+147.3101\left(\frac{l}{100}\right)^6-34.5437\left(\frac{l}{100}\right)^7. \qquad (3.10)\end{aligned}$$

IV. Discussion

By identifying the relevant cosmological parameters we have developed a fast ($\ll 1\,\mathrm{sec}$) and accurate (few percent or better) algorithm for computing the shape (C_l/C_2) of the tensor angular power spectrum for a primordial tensor power spectrum of the form

$$P_T(k) \propto (k\tau_0)^{n_T}k^{-3}, \qquad (4.1)$$

where τ_0 is the conformal time today. Our algorithm employs a polynomial in the parameters Ω_Λ, $\Omega_0 h^2$, $\Omega_B h^2$, n_T, and N_ν.

To assess the accuracy of our algorithm we sampled the following parameter intervals uniformly and at random: $0.35 \le h \le 0.8$, $2 \le N_\nu \le 12$, $0.005 \le \Omega_B h^2 \le 0.03$, $-0.3 \le n_T \le 0$, and $0 \le \Omega_\Lambda \le 0.8$. In Figs. 2 and 3 we show the histograms of the **maximum error** in C_l/C_2 for $\Omega_\Lambda = 0$ and $\Omega_\Lambda \neq 0$ respectively. For $\Omega_\Lambda = 0$ the maximum error (relative to the Boltzmann code of Ref. [10]) is less than about 0.5% for $l \le 50$ and less than about 2% for $l \le 100$. For $\Omega_\Lambda \neq 0$, the accuracy is slightly worse, better than about 1% for $l \le 50$ and better than about 3% for $l \le 100$. In the case of $\Omega_\Lambda \neq 0$ the largest errors occur for $\Omega_0 h^2 < 0.05$ (large Ω_Λ and small h).

The tensor contribution to the quadrupole plays a special role. It provides a convenient overall normalization for the angular power spectrum and can be related to the value of the inflationary potential when the comoving scale $k_* = H_0$ crossed outside the horizon during inflation [9]:

$$V_*/m_{\rm Pl}^4 = 0.66 \left[1. - (f_T^{(1)} + 0.1) n_T\right] \, C_2/f_T^{(0)}, \tag{4.2}$$

where the functions $f_T^{(0,1)}(\Omega_\Lambda)$ are given by

$$\begin{aligned} f_T^{(0)}(\Omega_\Lambda) &= 1. - 0.03\Omega_\Lambda - 0.1\Omega_\Lambda^2 \\ f_T^{(1)}(\Omega_\Lambda) &= 0.58 - 0.50\Omega_\Lambda + 0.31\Omega_\Lambda^2 - 0.88\Omega_\Lambda^3. \end{aligned} \tag{4.3}$$

The dependence of this relationship on cosmological parameters other than Ω_Λ is much less significant [9].

There is even more motivation for developing a fast and accurate algorithm for the scalar angular power spectrum. However, this task is more challenging: the power spectrum has more structure (cf., Fig. 1) and that structure extends to higher multipoles. We are currently working on an algorithm for the scalar angular power spectrum.

Acknowledgments

This work was supported by the DOE (at Chicago and at Fermilab) and by the NASA through Grant NAG5-2788.

References

[1] For a textbook discussion of inflation see e.g., E. W. Kolb and M. S. Turner, *The Early Universe* (Addison-Wesley, Redwood City, CA, 1990), Ch. 8, or A.D. Linde, *Inflation and Quantum Cosmology* (Academic Press, San Diego, CA, 1990).

[2] A. H. Guth and S.-Y. Pi, *Phys. Rev. Lett.* **49**, 1110 (1982); S. W. Hawking, *Phys. Lett. B* **115**, 295 (1982); A. A. Starobinskii, *ibid* **117**, 175 (1982); J. M. Bardeen, P. J. Steinhardt, and M. S. Turner, *Phys. Rev. D* **28**, 697 (1983).

[3] V.A. Rubakov, M. Sazhin, and A. Veryaskin, *Phys. Lett. B* **115**, 189 (1982); R. Fabbri and M. Pollock, *ibid* **125**, 445 (1983); A.A. Starobinskii *Sov. Astron. Lett.* **9**, 302 (1983); L. Abbott and M. Wise, *Nucl. Phys. B* **244**, 541 (1984); D.H. Lyth, *Phys. Rev. D* **31**, 1792 (1985).

[4] N. Sugiyama, astro-ph/9412025, *Astrophys. J. Suppl.*, in press.

[5] E.J. Copeland, E.W. Kolb, A.R. Liddle, and J.E. Lidsey, *Phys. Rev. Lett.* **71**, 219 (1993); *Phys. Rev. D* **48**, 2529 (1993); M.S. Turner, *ibid*, 3502 (1993); *ibid* **48**, 5539 (1993); A.R. Liddle and M.S. Turner, *Phys. Rev. D* **50**, 758 (1994).

[6] L. Knox, *Phys. Rev. D* **52**, 4307 (1995); G. Jungman, M. Kamionkowski, A. Kosowsky, and D.N. Spergel, astro-ph/9507080 (1995); G. Jungman et al., astro-ph/9512nnn.

[7] L. Kofman and A.A. Starobinskii, *Sov. Astron. Lett.* **11**, 271 (1985). **48**, 4613, (1993); M.S. Turner, M. White, J.E. Lidsey, *Phys. Rev. D* **48**, 4613 (1993); K.-W. Ng and A.D. Speliotopoulos, Phys. Rev. **D52**, 2112 (1995); Y. Wang, *Phys. Rev. D*, in press.

[8] B. Allen and S. Koranda, *Phys. Rev. D* **52**, 1902 (1995).

[9] M.S. Turner and M. White, astro-ph/9512nnn.

[10] S. Dodelson, L. Knox, and E. Kolb, *Phys. Rev. Lett.* **72**, 3444-7 (1994).

[11] See e.g., B.J.T. Jones and R.F.G. Wyse, *Astron. Astrophys.* **149**, 144 (1985).

Appendix A: Table of standard C_l's

l	$\frac{l(l+1)C_l(\Omega_\Lambda=0)}{6C_2(\Omega_\Lambda=0)}$	$\frac{l(l+1)C_l(\Omega_\Lambda=0.5)}{6C_2(\Omega_\Lambda=0.5)}$
2	1.000000000	1.000000000
3	7.85882861E-01	8.12787313E-01
4	7.43475686E-01	7.75447410E-01
5	7.35658928E-01	7.69590303E-01
6	7.38104089E-01	7.73328636E-01
7	7.43851511E-01	7.80190352E-01
8	7.50438650E-01	7.87827791E-01
9	7.56898572E-01	7.95302374E-01
10	7.62844076E-01	8.02234328E-01
11	7.68121692E-01	8.08471560E-01
12	7.72700749E-01	8.13985567E-01
13	7.76567875E-01	8.18762161E-01
14	7.79782672E-01	8.22865837E-01
15	7.82327767E-01	8.26275290E-01
16	7.84314505E-01	8.29111207E-01
17	7.85671940E-01	8.31292902E-01
18	7.86573958E-01	8.33010933E-01
19	7.86864814E-01	8.34090814E-01
20	7.86805032E-01	8.34819817E-01
21	7.86129624E-01	8.34902088E-01
22	7.85208901E-01	8.34747737E-01
23	7.83648115E-01	8.33916120E-01
24	7.81949251E-01	8.32965076E-01
25	7.79570004E-01	8.31288581E-01
26	7.77161094E-01	8.29611689E-01
27	7.74020055E-01	8.27148151E-01
28	7.70959238E-01	8.24805533E-01
29	7.67105366E-01	8.21604444E-01
30	7.63442668E-01	8.18647318E-01
31	7.58920711E-01	8.14753604E-01
32	7.54699914E-01	8.11226404E-01
33	7.49551094E-01	8.06680893E-01
34	7.44812364E-01	8.02623603E-01
35	7.39076276E-01	7.97464933E-01
36	7.33855970E-01	7.92913085E-01
37	7.27571031E-01	7.87178514E-01
38	7.21903458E-01	7.82165288E-01
39	7.15107322E-01	7.75891111E-01
40	7.09025177E-01	7.70447667E-01

l	$\frac{l(l+1)C_l(\Omega_\Lambda=0)}{6C_2(\Omega_\Lambda=0)}$	$\frac{l(l+1)C_l(\Omega_\Lambda=0.5)}{6C_2(\Omega_\Lambda=0.5)}$
41	7.01754819E-01	7.63669098E-01
42	6.95290317E-01	7.57825769E-01
43	6.87581696E-01	7.50576759E-01
44	6.80766517E-01	7.44363318E-01
45	6.72655788E-01	7.36677916E-01
46	6.65520307E-01	7.30122320E-01
47	6.57043916E-01	7.22034754E-01
48	6.49618128E-01	7.15164612E-01
49	6.40812380E-01	7.06709069E-01
50	6.33125395E-01	6.99550707E-01
51	6.24026867E-01	6.90761689E-01
52	6.16107568E-01	6.83341454E-01
53	6.06751841E-01	6.74252272E-01
54	5.98629552E-01	6.66596862E-01
55	5.89051404E-01	6.57240302E-01
56	5.80754839E-01	6.49375955E-01
57	5.70988919E-01	6.39784406E-01
58	5.62546297E-01	6.31736935E-01
59	5.52626894E-01	6.21943006E-01
60	5.44065284E-01	6.13736759E-01
61	5.34026679E-01	6.03773187E-01
62	5.25372061E-01	5.95432062E-01
63	5.15247817E-01	5.85331082E-01
64	5.06526007E-01	5.76878240E-01
65	4.96347985E-01	5.66670612E-01
66	4.87585435E-01	5.58131161E-01
67	4.77383343E-01	5.47844948E-01
68	4.68606069E-01	5.39242990E-01
69	4.58408817E-01	5.28906521E-01
70	4.49640932E-01	5.20265325E-01
71	4.39477440E-01	5.09906642E-01
72	4.30741650E-01	5.01246850E-01
73	4.20639523E-01	4.90893728E-01
74	4.11958163E-01	4.82237697E-01
75	4.01942685E-01	4.71915135E-01
76	3.93337874E-01	4.63283465E-01
77	3.83432932E-01	4.53015076E-01
78	3.74925150E-01	4.44428914E-01
79	3.65153926E-01	4.34239289E-01
80	3.56761877E-01	4.25716630E-01

l	$\frac{l(l+1)C_l(\Omega_\Lambda=0)}{6C_2(\Omega_\Lambda=0)}$	$\frac{l(l+1)C_l(\Omega_\Lambda=0.5)}{6C_2(\Omega_\Lambda=0.5)}$
81	3.47146488E-01	4.15627684E-01
82	3.38887429E-01	4.07185415E-01
83	3.29449095E-01	3.97220535E-01
84	3.21338323E-01	3.88874768E-01
85	3.12097094E-01	3.79055720E-01
86	3.04149866E-01	3.70821411E-01
87	2.95121515E-01	3.61164479E-01
88	2.87354633E-01	3.53060287E-01
89	2.78552720E-01	3.43581079E-01
90	2.70980245E-01	3.35623379E-01
91	2.62418690E-01	3.26338036E-01
92	2.55052066E-01	3.18539155E-01
93	2.46743720E-01	3.09462129E-01
94	2.39593392E-01	3.01833443E-01
95	2.31549532E-01	2.92978236E-01
96	2.24624559E-01	2.85530583E-01
97	2.16855038E-01	2.76910111E-01
98	2.10163325E-01	2.69653750E-01
99	2.02676236E-01	2.61279304E-01
100	1.96225065E-01	2.54224121E-01

Appendix B: Last Scattering

In the early Universe, matter and radiation were in good thermal contact, because of the rapid interactions between the photons and electrons. As the temperature dropped below 0.3eV, electrons combined with protons to form neutral hydrogen ("recombination") at a redshift of around 1300. With the disappearance of free electrons, the photon mean free path became very large ($> H^{-1}$) and matter and radiation decoupled at a redshift of around 1100. Last scattering is crucial in calculating the CBR anisotropy. [11]

The redshift of last scattering, $z_{\rm LSS}$, is given by the peak of the visibility function $g(z) \equiv e^{-\tau}{\rm d}\tau/{\rm dz}$; $g(z){\rm d}z$ measures the probability that a given photon suffered its last scattering in the redshift interval (z, z+dz). The optical depth (measured from the

present back to redshift z) is given by

$$\tau(z) = c \int_0^z \mathrm{d}z \frac{\mathrm{d}t}{\mathrm{d}z} n_e(z)\, \sigma_T, \tag{6.1}$$

where $\mathrm{d}t$ is the proper time interval, $n_e(z)$ is the electron number density, and $\sigma_T = 6.65 \times 10^{-25}\,\mathrm{cm}^2$ is the Thomson scattering cross-section. The electron number density depends on $\Omega_B h^2$ and $H(t)$, the Hubble parameter at time t. At the relevant times (around recombination and last scattering), $H(t)$ only depends on $\Omega_0 h^2$ and N_ν. Hence, $z_{\rm LSS}$ only depends on $\Omega_B h^2$, $\Omega_0 h^2$, and N_ν. Numerically, we find

$$z_{\rm LSS} = 1104.37 + \Delta z(\Omega_B h^2, \Omega_0 h^2) + \Delta z(\Omega_0 h^2) + \Delta z(N_\nu, \Omega_B h^2, \Omega_0 h^2), \tag{6.2}$$

where

$$\begin{aligned}
\Delta z(\Omega_B h^2, \Omega_0 h^2) &= 0.5285 \left[(\Omega_B h^2)^{-1} - 0.0125^{-1}\right] \left(\frac{\Omega_0 h^2}{0.25}\right)^{0.31} \\
&\quad - 7.022 \times 10^{-4} \left[(\Omega_B h^2)^{-1} - 0.0125^{-1}\right]^2 \left(\frac{\Omega_0 h^2}{0.25}\right)^{0.55} \\
\Delta z(\Omega_0 h^2) &= 73.21 \left[\sqrt{\Omega_0 h^2} - 0.5\right] - 12.06 \left[\sqrt{\Omega_0 h^2} - 0.5\right]^2 \\
\Delta z(N_\nu, \Omega_B h^2, \Omega_0 h^2) &= 0.3823 (N_\nu - 3) \left(\frac{\Omega_B h^2}{0.0125}\right)^{-0.756} \left(\frac{\Omega_0 h^2}{0.25}\right)^{-0.46}.
\end{aligned} \tag{6.3}$$

Our fitting formula is accurate to $\Delta z = \pm 1$ for the parameter ranges of $0.1 \leq \Omega_0 h^2 \leq 0.64$, $0.005 \leq \Omega_B h^2 \leq 0.03$, and $2 \leq N_\nu \leq 12$.

Figure Captions

Fig.1 The predicted scalar and tensor contributions. The set of cosmological parameters is: $h = 0.5$, $\Omega_B = 0.05$, $N_\nu = 3$, $\Omega_\Lambda = 0$, $n_T = 0$.

Fig.2 Histograms of maximum error for $l \leq 50$ and $l \leq 100$ ($\Omega_\Lambda = 0$).

Fig.3 Histograms of maximum error for $l \leq 50$ and $l \leq 100$ ($\Omega_\Lambda > 0$).

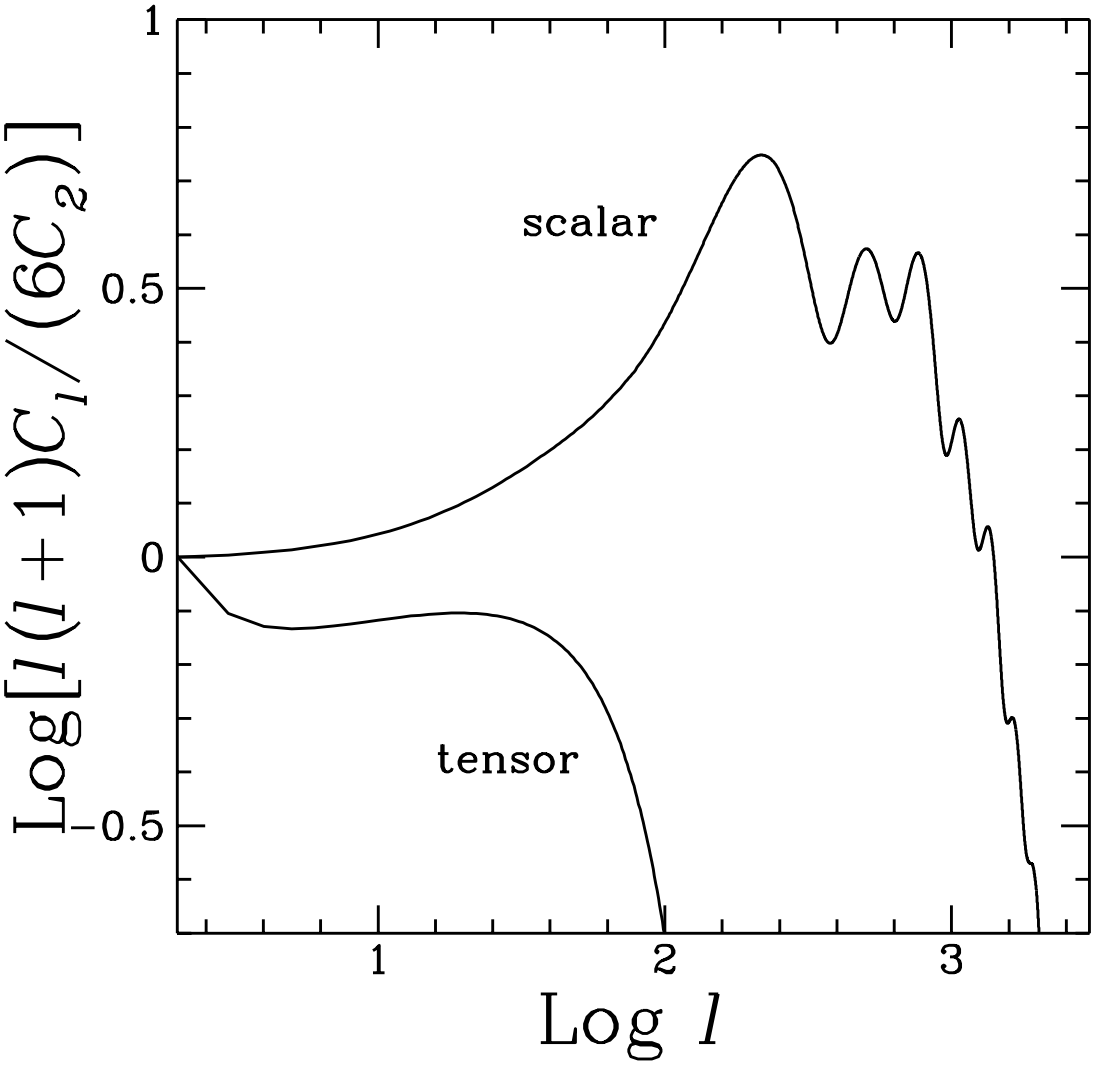

Figure 1: The predicted scalar and tensor contributions. The set of cosmological parameters is: $h = 0.5$, $\Omega_B = 0.05$, $N_\nu = 3$, $\Omega_\Lambda = 0$, $n_T = 0$.

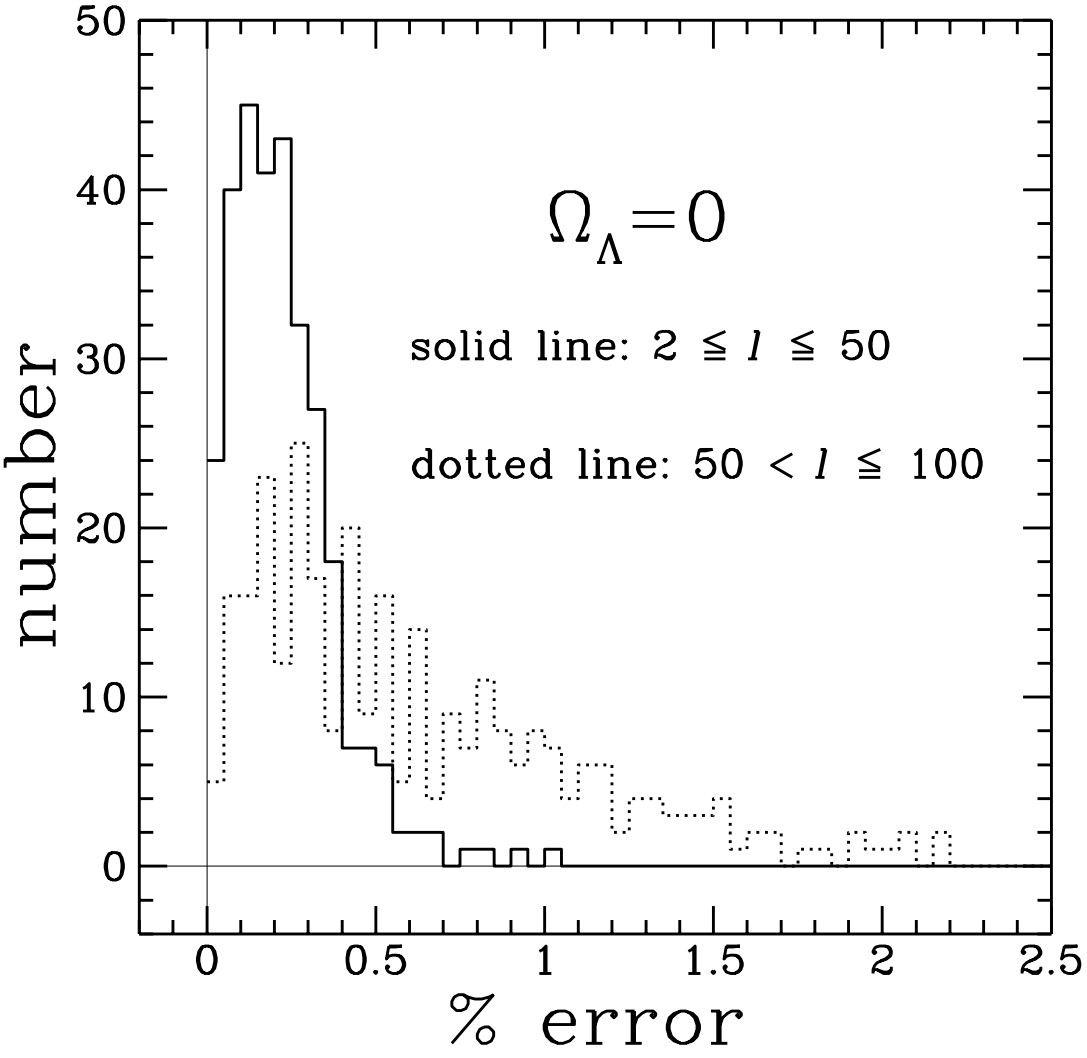

Figure 2: Histograms of maximum error for $l \leq 50$ and $l \leq 100$ ($\Omega_\Lambda = 0$).

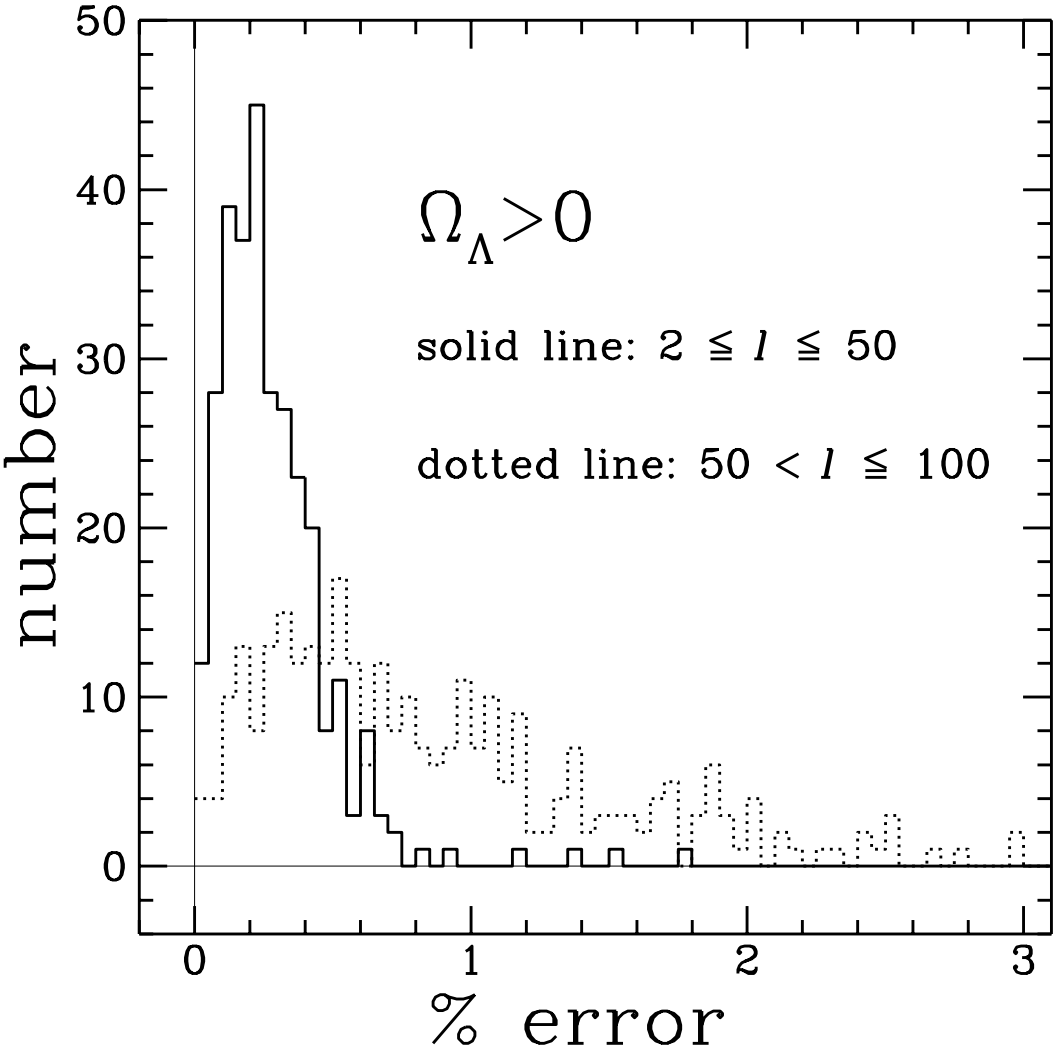

Figure 3: Histograms of maximum error for $l \leq 50$ and $l \leq 100$ ($\Omega_\Lambda > 0$).